

**Supporting Information for**  
**Two-dimensional spin-valley-coupled Dirac semimetals in**  
**functionalized SbAs monolayers**

Zhifeng Liu<sup>ab</sup>, Wangxiang Feng<sup>cd</sup>, Hongli Xin<sup>a</sup>, Yinlu Gao<sup>e</sup>, Pengfei Liu<sup>bf</sup>,  
Yugui Yao<sup>c</sup>, Hongming Weng<sup>gh</sup>, Jijun Zhao<sup>be\*</sup>

<sup>a</sup>*School of Physical Science and Technology, Inner Mongolia University, Hohhot  
010021, China*

<sup>b</sup>*Beijing Computational Science Research Center, Beijing 100094, China*

<sup>c</sup>*School of Physics, Beijing Institute of Technology, Beijing 100081, China*

<sup>d</sup>*Peter Grünberg Institut and Institute for Advanced Simulation, Forschungszentrum  
Jülich and JARA, 52425 Jülich, Germany*

<sup>e</sup>*Key Laboratory of Materials Modification by Laser, Ion and Electron Beams (Dalian  
University of Technology), Ministry of Education, Dalian 116024, China*

<sup>f</sup>*Institute of High Energy Physics, Chinese Academy of Sciences (CAS), Beijing  
100049, China*

<sup>g</sup>*Beijing National Laboratory for Condensed Matter Physics and Institute of Physics,  
Chinese Academy of Sciences, Beijing 100190, China*

<sup>h</sup>*Songshan Lake Materials Laboratory, Guangdong 523808, China*

- I. Mechanical exfoliation for SbAs ML
- II. Structure and stability of freestanding SbAs ML
- III. Band structures of SbAs ML
- IV. Band structures of SbAsH<sub>2</sub> ML
- V. Band structures of SbAsX<sub>2</sub> (X=F, Cl, Br and I) MLs
- VI. Band structure of 2.3-SbAsH<sub>2</sub> ML from HSE06
- VII. svc-DSM states of SbAsX<sub>2</sub> (X=F, Cl, Br and I) MLs
- VIII. Strain induced band inversion

## I. Mechanical exfoliation for SbAs ML

Since the layered structure of bulk SbAs [see Figs. S1(a) and S1(b)] has been synthesized in experiment, we calculate the cleavage energy by introducing a fracture in it so as to examine whether the SbAs ML can be obtained from the bulk sample via mechanical exfoliation in experiment. As shown in Fig. S1(c), the calculated cleavage energy quickly increases with the increasing separation distance ( $d-d_0$ ) and then saturates to a value corresponding to the exfoliation energy about  $0.34 \text{ J/m}^2$ . For comparison, the cleavage energies of some representative layered materials (e.g., graphite, h-BN and  $\text{MoS}_2$ ) have also been calculated [see Fig. S1(d)]. Remarkably, the  $0.34 \text{ J/m}^2$  exfoliation energy of SbAs is smaller than that of the famous graphite ( $0.38 \text{ J/m}^2$ ) and h-BN ( $\sim 0.51 \text{ J/m}^2$ ), suggesting that it is feasible to obtain the SbAs ML by mechanical exfoliation from the existing bulk like the graphene. It should be noted that the reliability of our calculated results can be confirmed by the agreement between our results and the previous data, such as  $0.38 \text{ J/m}^2$  versus  $0.37 \text{ J/m}^2$  [1] for graphite, and  $0.29 \text{ J/m}^2$  versus  $0.27 \text{ J/m}^2$  [2] for  $\text{MoS}_2$ .

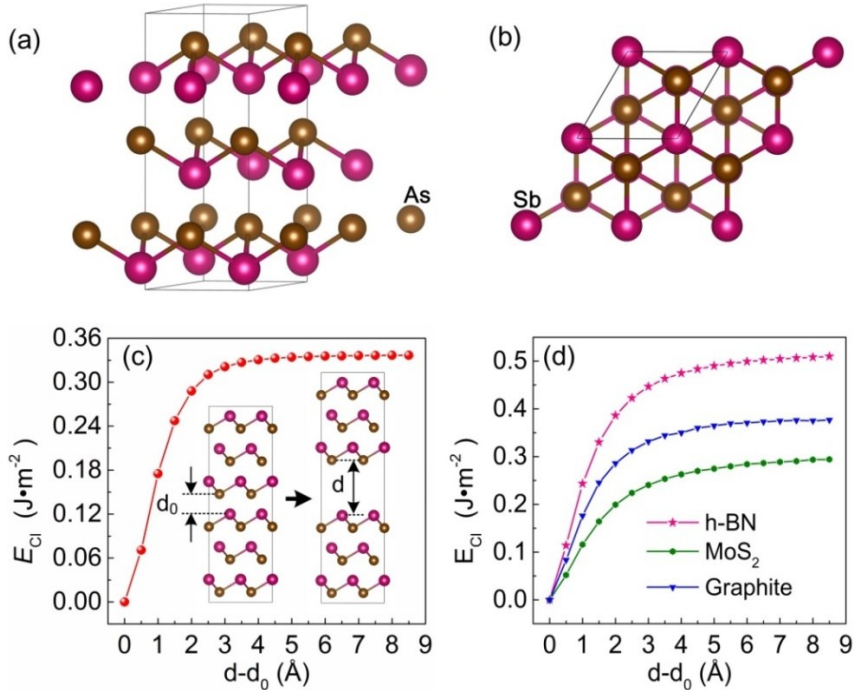


FIG. S1. (a) Side and (b) top view of the optimized atomic structure for the chemical ordered SbAs solid. (c) Cleavage energy  $E_{\text{cl}}$  as a function of the separation distance  $d-d_0$  between two fractured parts of layered SbAs. For comparison, the corresponding (d) cleavage energy of layered h-BN,  $\text{MoS}_2$  and graphite are also presented.

## II. Structure and stability of freestanding SbAs ML

As shown in Figs. S2(a) and S2(b), the optimized atomic structure of pristine SbAs ML is buckled as the case of silicene [3], which derives from the relatively weak bonding between Sb and As atoms. Such buckling is benefit to enhance the overlap between  $\pi$  and  $\sigma$  orbitals and stabilizes the system. Its dynamical and thermal stability has been respectively confirmed by our phonon calculation that shows non imaginary frequencies [Fig. S2(c)], and *ab initio* molecular dynamic (AIMD) simulation in which there are no structural destruction [Fig. S2(d)].

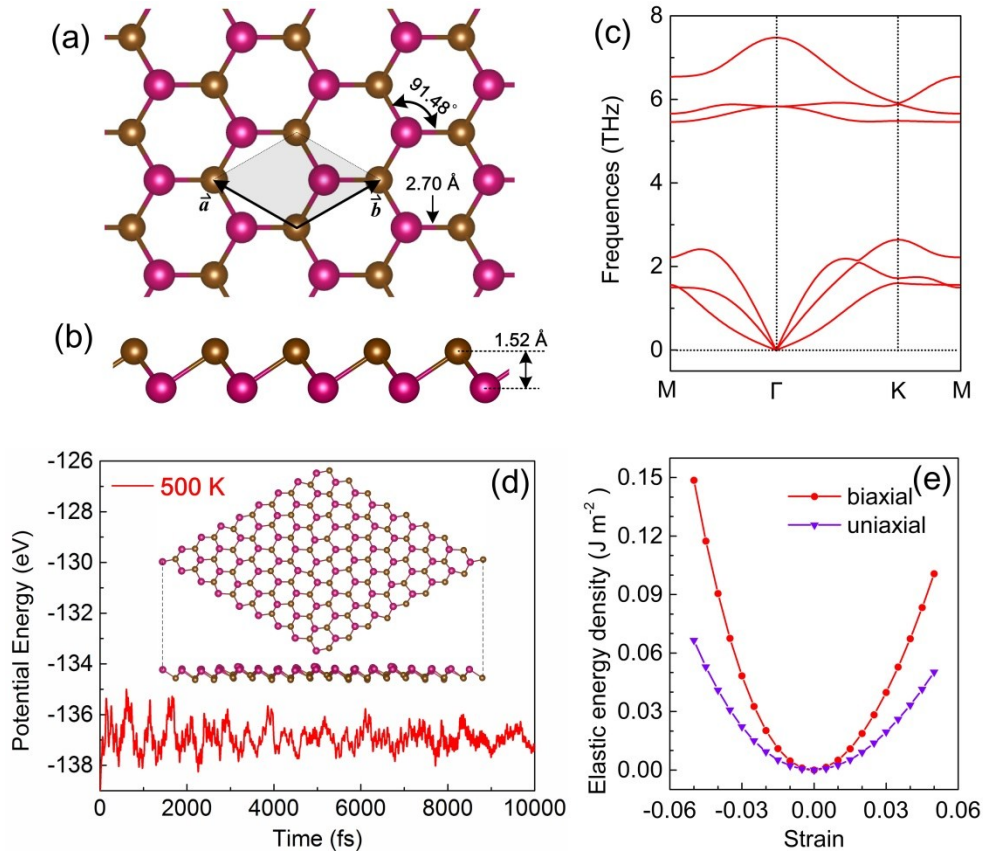


FIG. S2. Top (a) and side (b) views of optimized structure, phonon dispersion (c), total potential energy fluctuation (d) during the AIMD simulations at 500K, and strain energies under different biaxial and uniaxial strains for SbAs ML. The inset in (d) shows the snapshot at the end of simulation of 10 ps.

In experiment, the chemical functionalization of SbAs ML requires that the exfoliated SbAs ML should be able to withstand its own weight and form a freestanding membrane. To check this aspect, we calculate the in-plane stiffness of

the SbAs ML characterized by in-plane Young's modulus  $Y_{2D}$ , which is defined as

$$Y_{2D} = \frac{C_{11}^2 - C_{12}^2}{C_{11}}, \quad (1)$$

where  $C_{11}$  and  $C_{12}$  is the corresponding linear elastic constants. For 2D materials, the elastic energy density  $U(\varepsilon)$  can be expressed as [4]:

$$U(\varepsilon) = \frac{1}{2}C_{11}\varepsilon_{xx}^2 + \frac{1}{2}C_{22}\varepsilon_{yy}^2 + C_{12}\varepsilon_{xx}\varepsilon_{yy} + 2C_{44}\varepsilon_{xy}^2. \quad (2)$$

Thus, the elastic constants of  $C_{11}$ ,  $C_{12}$  can be derived by fitting the curves of  $U(\varepsilon)$  with respect to uniaxial and equi-biaxial strain [Fig. S2 (e)]. The  $Y_{2D}$  of SbAs ML is calculated to be 46.4 GPa·nm. On the basis of the calculated  $Y_{2D}$ , the gravity induced typical out-of-plane deformation  $h$  can be estimated by [5]

$$\frac{h}{l} = \left(\frac{\sigma gl}{Y_{2D}}\right)^{1/3}, \quad (3)$$

where  $\sigma$  ( $=2.53 \times 10^{-6}$  Kg/m<sup>2</sup>) is the surface density of SbAs ML,  $l$  is the size of possible free-standing SbAs flakes. If we assume a macroscopic size  $l \approx 100$   $\mu$ m, the  $h/l$  is calculated to be  $3.76 \times 10^{-4}$ . This value is of the same order of magnitude as that of graphene [5]. This indicates that without the support of a substrate, the in-plane stiffness of SbAs ML is strong enough to withstand its own weight and keep its free-standing membrane.

### III. Band structure of SbAs ML

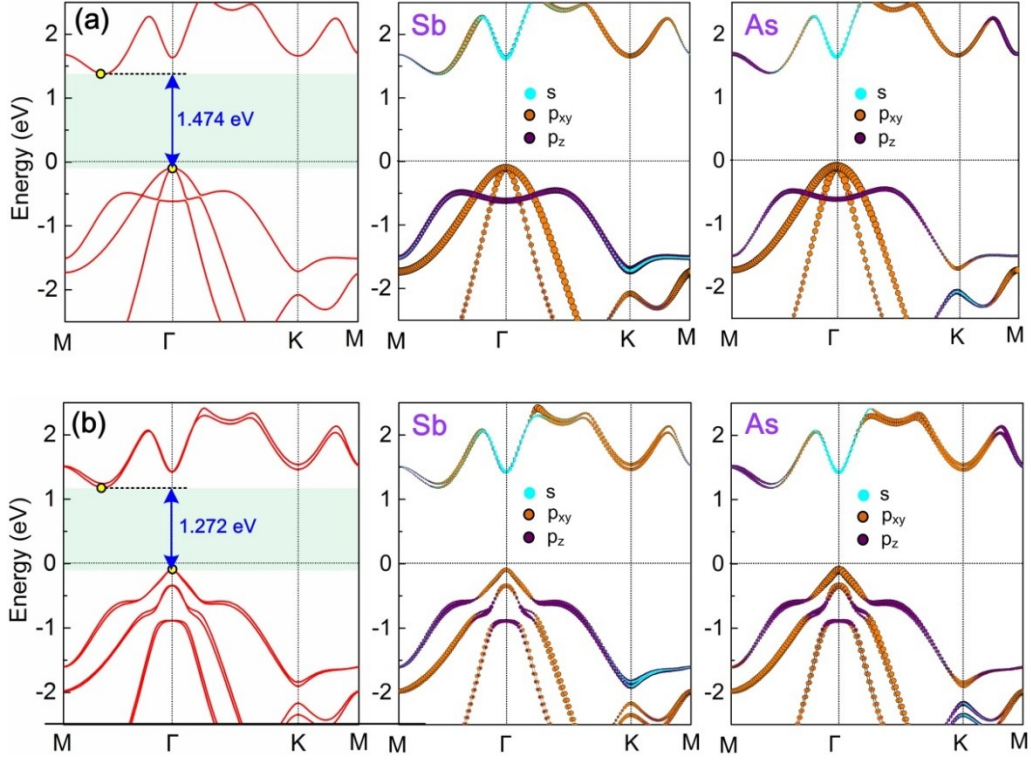


FIG. S3. Electronic band structures of SbAs ML (a) without SOC and (b) with SOC. The corresponding orbital-resolved electronic band structures for Sb and As atoms are displayed at the same row. Clearly, SbAs ML is an indirect semiconductor. The valence band maximum (VBM) at  $\Gamma$  point is mainly contributed by hybridization of  $\text{Sb-}p_{xy}$  and  $\text{As-}p_{xy}$  states, while the conduction band minimum (CBM) at the origin originates from  $\text{Sb-}p_z$  and  $\text{As-}p_z$  states, as well as few contribution of  $s$  state. Note that at the higher-lying valence band, the contribution of  $p_z$  for both Sb and As is obvious. When the SOC effect is considered, the spin-splitting at CBM leads to a distinct decrease in band gap (from 1.474 eV to 1.272 eV).

#### IV. Band structure of SbAsH<sub>2</sub> ML

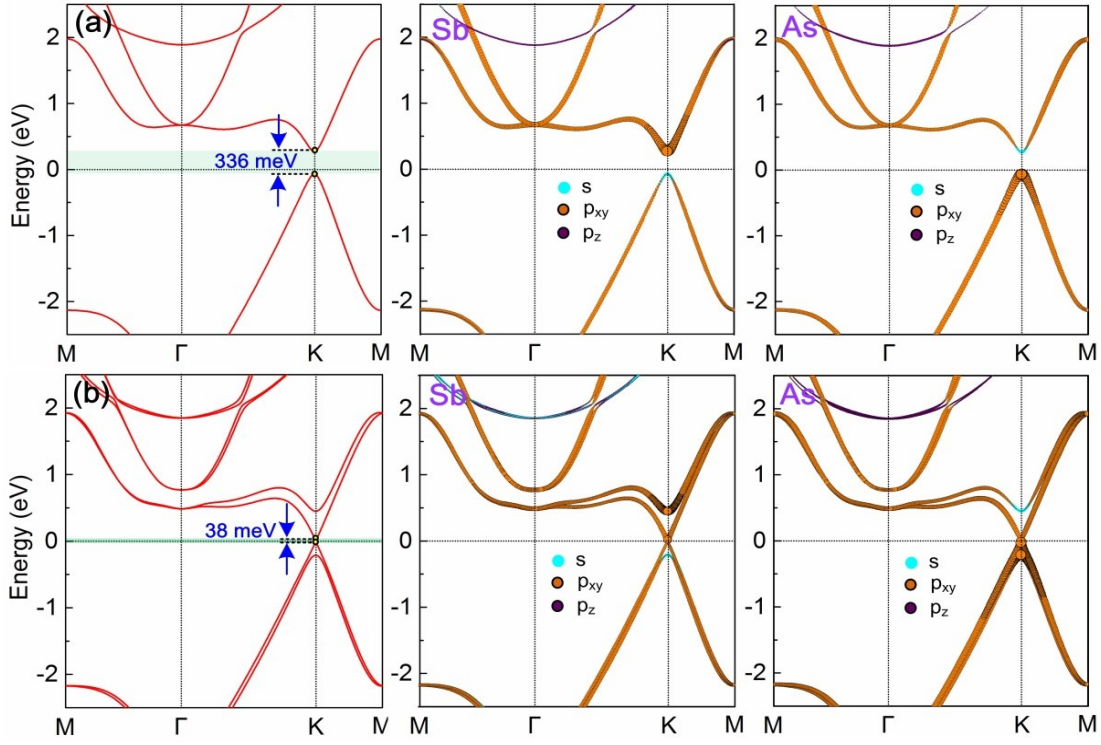


FIG. S4. Electronic band structures of SbAsH<sub>2</sub> ML (a) without SOC and (b) with SOC. The corresponding orbital-resolved electronic band structures for Sb and As atoms are displayed at the same row. Unlike the case of SbAs ML, SbAsH<sub>2</sub> is a direct semiconductor with greatly reduced band gap at K point. Since the electronegativity of H atom is larger than that of both Sb and As atoms, the  $p_z$  electrons of the SbAs ML transfer to the functional group H atoms. Thus the Fermi level moves down, and the  $p_z$  states of SbAs ML strongly couple with the H-s state at the deep energy level. As shown in the figure, the  $p_z$  state is almost no contribution to both valence and conduction bands in the vicinity of new Fermi level for SbAsH<sub>2</sub>. The VBM is mainly contributed by Sb- $p_{xy}$  and As-s orbitals, while the main contribution of CBM is Sb-s and As- $p_{xy}$  orbitals. Interestingly, in the present of SOC, giant spin-splitting can be found at the inversion asymmetric K point, which leads to a further reduced band gap (38 meV).

## V. Band structures of $\text{SbAsX}_2$ ( $X=\text{F, Cl, Br and I}$ ) ML

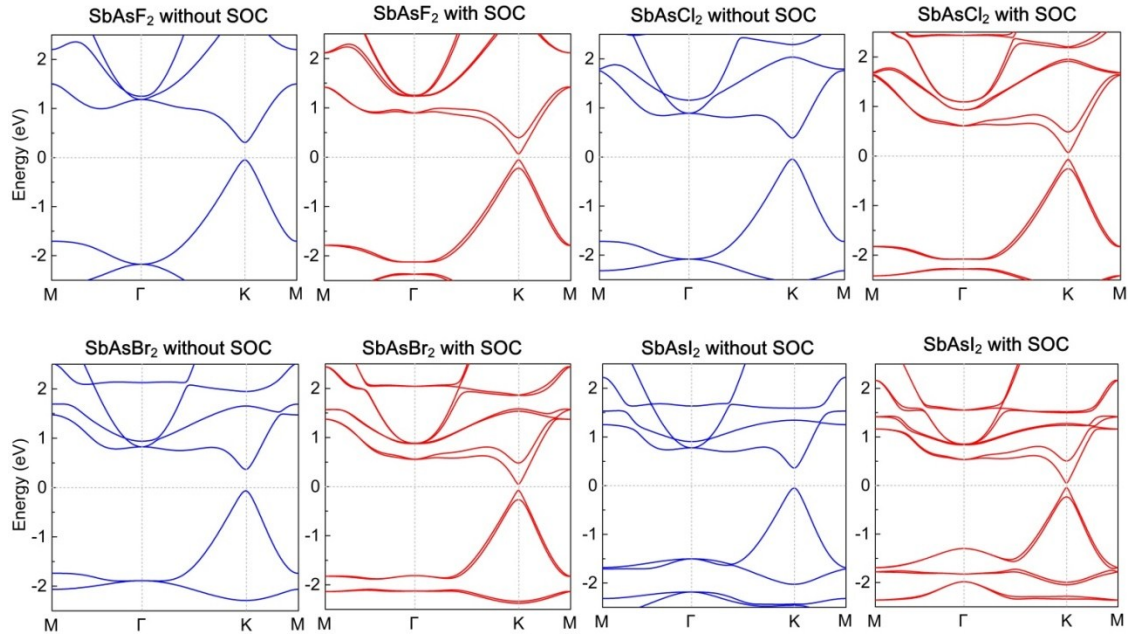


FIG. S5. Electronic band structures of  $\text{SbAsX}_2$  ( $X=\text{F, Cl, Br and I}$ ) without SOC and with SOC. The distribution of orbitals is similar with the case of  $\text{SbAsH}_2$  (see Fig. S4)

## VI. Band structure of 2.3-SbAsH<sub>2</sub> ML from HSE06

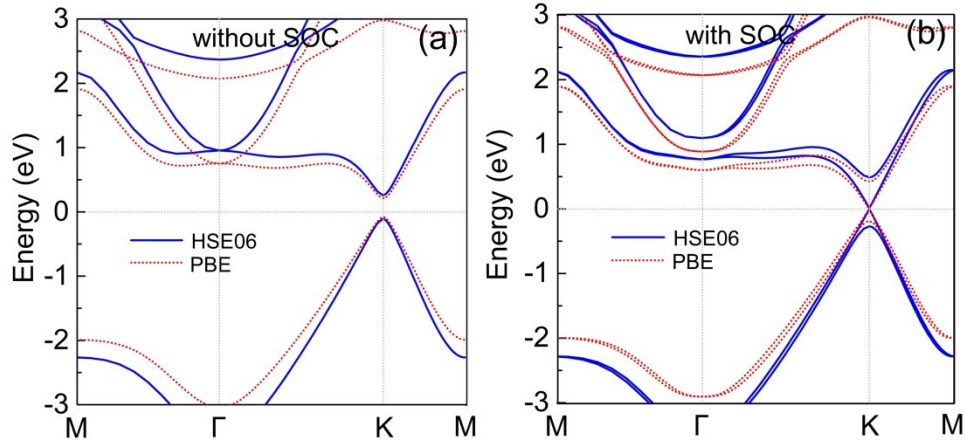


FIG. S6. The band structure (blue solid line) calculated from HSE06 method (a) without SOC and (b) with SOC for the 2.3-SbAsH<sub>2</sub> ML. For comparison, the bands at PBE theory level are also displayed (red dashed line). Although the positions of most bands show relative shifts in these two methods, those of VBM and CBM at K point stay still. Thus, the spin-splitting Dirac state is well preserved, confirming that the 2.3-SbAsH<sub>2</sub> is indeed a Dirac semimetal.

## VII. svc-DSM state of $\text{SbAsX}_2$ ( $X=\text{F, Cl, Br}$ and $\text{I}$ ) MLs

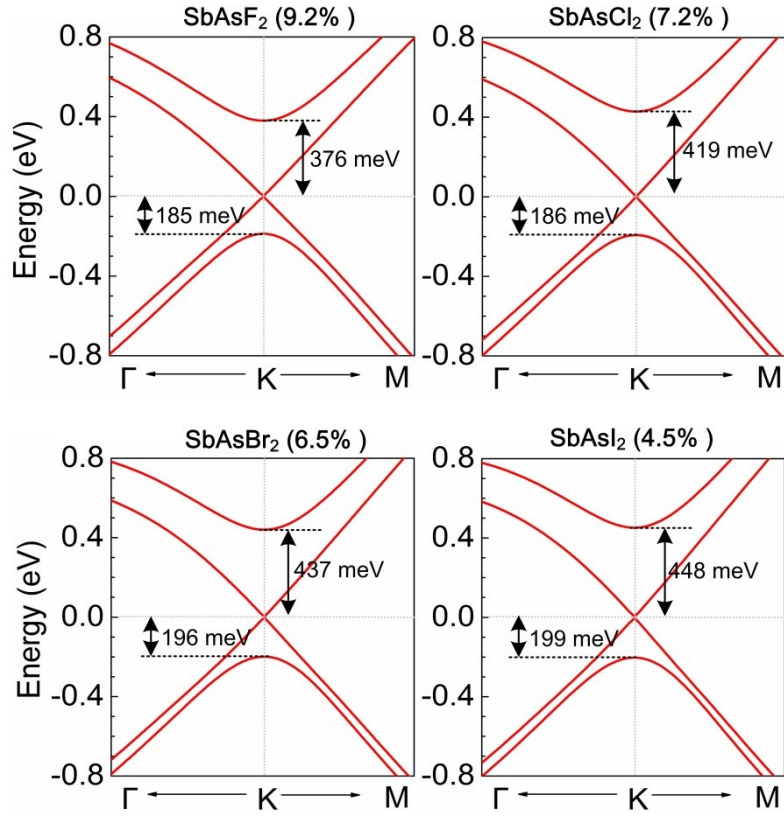


FIG. S7. The enlarged band structure with SOC near the Fermi level around the K point for  $\text{SbAsX}_2$  ( $X=\text{F, Cl, Br}$  and  $\text{I}$ ) MLs under critical strain. Clearly, similar to  $\text{SbAsH}_2$ , the svc-DSM state is formed in the critical strain for all the other  $\text{SbAsX}_2$  MLs.

### VIII. Strain induced band inversion

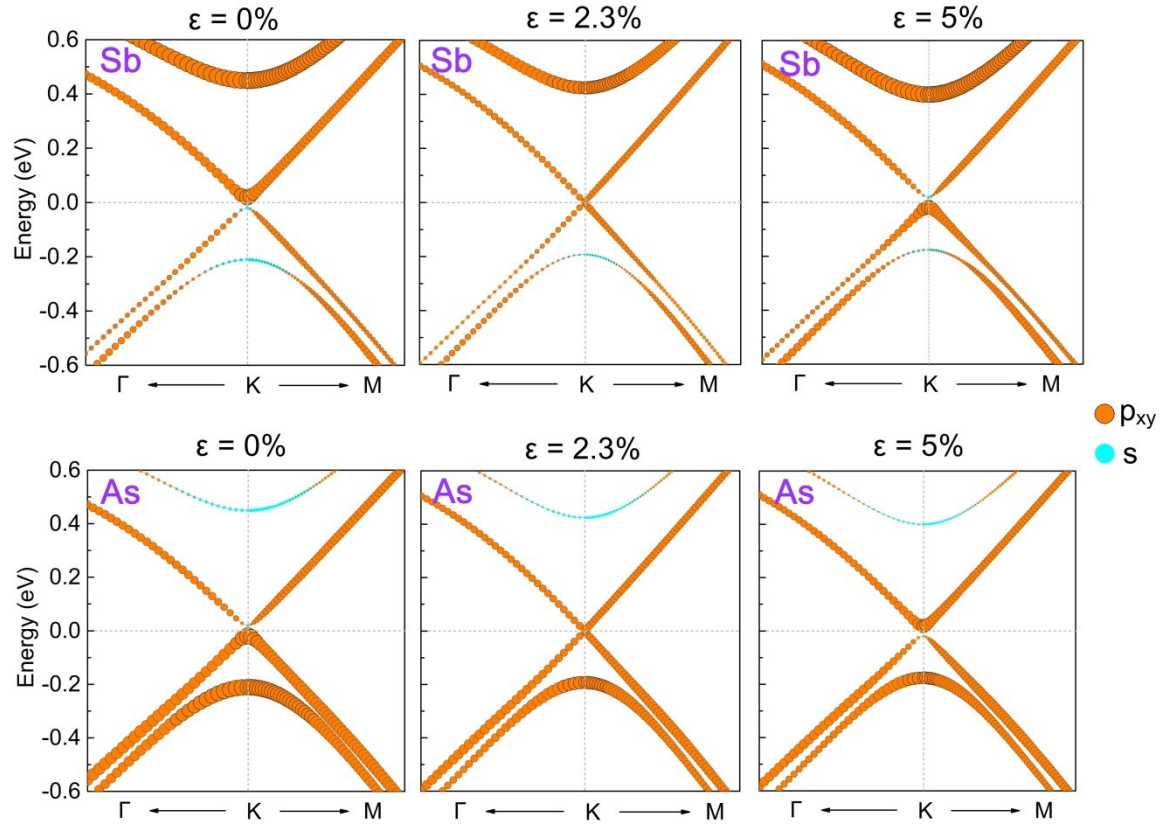


FIG. S8. The orbital-resolved band structures in the vicinity of Fermi level for Sb and As atoms of SbAsH<sub>2</sub> ML with zero, 2.3% and 5% tensile strain.

## References

- [1] Zacharia, R.; Ulbricht, H.; Hertel, T. Interlayer cohesive energy of graphite from thermal desorption of polyaromatic hydrocarbons. *Phys. Rev. B* **2004**, *69*, 155406.
- [2] Björkman, T.; Gulans, A.; Krasheninnikov, A. V.; Nieminen, R. M. van der Waals bonding in layered compounds from advanced density-functional first-principles calculations. *Phys. Rev. Lett.* **2012**, *108*, 235502.
- [3] Cahangirov, S.; Topsakal, M.; Akturk, E.; Sahin, H.; Ciraci, S. Two- and one-dimensional honeycomb structures of silicon and germanium. *Phys. Rev. Lett.* **2009**, *102*, 236804.
- [4] Andrew, R. C.; Mapasha, R. E.; Ukpong, A. M.; Chetty, N. Mechanical properties of graphene and boronitrene. *Phys. Rev. B* **2012**, *85*, 125428.
- [5] Booth, T. J.; Blake, P.; Nair, R. R.; Jiang, D.; Hill, E. W.; Bangert, U.; Bleloch, A.; Gass, M.; Novoselov, K. S.; Katsnelson, M. I.; Geim, A. K. Macroscopic graphene membranes and their extraordinary stiffness. *Nano Lett.* **2008**, *8*, 2442-2446.